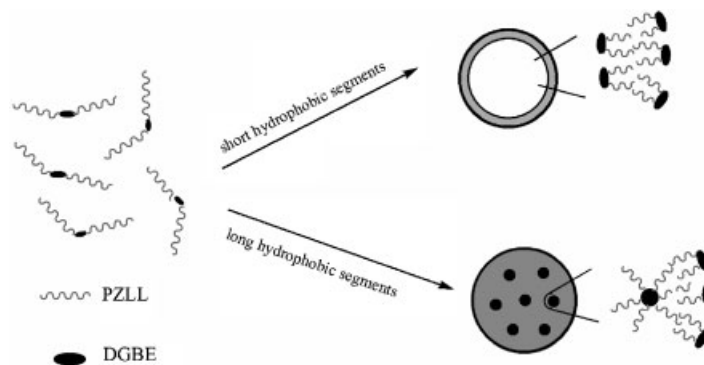


# Self-Assembly of a Hydrophobic Polypeptide Containing a Short Hydrophilic Middle Segment: Vesicles to Large Compound Micelles

Jing Sun, Quan Shi, Xuesi Chen, Jinshan Guo, Xiabin Jing\*

This report describes a facile route to prepare the vesicles and large compound micelles (LCMs) from a series of poly( $\epsilon$ -benzyloxycarbonyl L-lysine)-*block*-poly[diethylene glycol *bis*(3-amino propyl) ether]-*block*-poly( $\epsilon$ -benzyloxycarbonyl L-lysine) (PZLL-DGBE-PZLL) in their water solution, depending on molecular weight of the polypeptides. A pyrene probe is used to demonstrate the aggregate formation of PZLL-DGBE-PZLL in solution, and also to measure their critical micelle concentration as a function of molecular weight of the polymer. Transmission electron microscopy, atomic force microscopy, dynamic light scattering and confocal laser scanning microscopy are used to observe their aggregate morphologies. Rhodamine B is used as a fluorescent probe to confirm the structure of large compound micelles composed of many reverse micelles with aqueous cores. These polypeptides are prepared by ring-opening polymerization of  $\alpha$ -amino acid *N*-carboxyanhydrides with a small molecule as the initiator. Their structures are confirmed by NMR and SEC-MALLS. These vesicles and large compound micelles are extremely expected to be used in drug delivery.



## Introduction

Recently, there has been increasing interest in the design of a kind of novel macromolecules, not only exhibiting the characteristics of nano/micro-scale self-assembling, but also having good biocompatibility.<sup>[1–5]</sup> Proteins are neces-

sary for human beings to live. They are known to form  $\alpha$ -helices or  $\beta$ -sheets as their fundamental secondary motifs via intra- and intermolecular interactions between the functional groups of residual amino acids. Compared to natural proteins, synthetic polypeptides offer more advantages in stability and processability. Great efforts have been made to incorporate proteins or polypeptides into synthetic materials.<sup>[6–11]</sup> For example, recently: Akashi et al. reported a one-step preparation of polypeptide nanospheres with dual initiators in a mixture of water/DMSO,<sup>[12]</sup> Lecommandoux et al. studied stimuli-responsive vesicles from a peptide-based diblock copolymer polybutadiene-*block*-poly(L-glutamic acid) (PB-*b*-PGA),<sup>[13]</sup> Deming et al. demonstrated the charged polypeptide vesicles with promising biomimetic encapsulants,<sup>[14]</sup> and,

J. Sun, Q. Shi, X. Chen, J. Guo, X. Jing  
State Key Laboratory of Polymer Physics and Chemistry,  
Changchun Institute of Applied Chemistry, Chinese Academy of  
Sciences, Changchun 130022, P. R. China  
Fax: +86-431-85262775; E-mail: xbjing@ciac.jl.cn  
J. Sun, Q. Shi, J. Guo  
Graduate School of Chinese Academy of Sciences, Beijing, 100039,  
P. R. China

Kataoka et al. reported a kind of novel polyion complex micelles which can entrap enzyme molecules in aqueous media.<sup>[15]</sup>

In the 1990s, Eisenberg et al. found multiple morphologies formed by block copolymer polystyrene-*block*-poly(acrylic acid) (PS-PAA)<sup>[16]</sup> with different block lengths. One of these morphologies - "large compound micelles" (LCMs) - was reported for the first time. The LCMs were microscale spheres, which consisted of hydrophilic surface and reverse-micelle-like aggregates inside. Subsequently, LCMs were also observed for other copolymers with PS as the hydrophobic blocks, such as polystyrene-*block*-poly(ethylene oxide) (PS-*b*-PEO)<sup>[17]</sup> and polystyrene-*block*-poly(4-vinylpyridinium methyl iodide) (PS-*b*-P4VPMeI).<sup>[18]</sup> LCMs have a superficial resemblance to cells and also have great application potential in drug delivery.<sup>[16]</sup> They can entrap not only small molecule hydrophobic drugs but also hydrophilic drugs or proteins. Meanwhile, they may show some targeting mechanism: in a hydrophobic environment, such as in lipids, they may break down into many reverse micelles, and deliver hydrophobic drugs. Of course, for a drug delivery system, biocompatible and biodegradable carrier should be more practical.

In this study, we successfully prepared LCMs from a hydrophobic polypeptide with a hydrophilic small segment in the middle of it in a facile way. Although, there are many reports of polypeptide-synthetic polymer hybrid block copolymers,<sup>[19]</sup> to our knowledge, this is the first time this kind of morphology for polypeptides has been obtained. This polypeptide was prepared by ring-opening polymerization of  $\epsilon$ -benzyloxycarbonyl-L-lysine *N*-carboxyanhydride (ZLL NCA) with diethylene glycol bis(3-amino propyl) ether (DGBE) as initiator. Depending on its molecular weight, it could self-assemble into either vesicles or LCMs in aqueous solution.

## Experimental Part

### Materials

$\epsilon$ -Benzyloxycarbonyl L-lysine (ZLL) was purchased from GL Biochem (Shanghai) Ltd. Diethylene glycol bis(3-amino propyl) ether (DGBE) ( $\geq 98\%$ ) from Fluka was used without further purification. Dimethyl formamide (DMF) was dried over CaH<sub>2</sub> and distilled under vacuum before use. Tetrahydrofuran (THF) was dried and distilled in the presence of sodium prior to use.

### Synthesis of ZLL NCA

According to the method of Daly,<sup>[20]</sup> ZLL NCA was synthesized from ZLL and triphosgene in THF at 50 °C. After 1.5 h, the mixture was precipitated by petroleum ether, and then purified by three times of re-crystallization with ethyl acetate and petroleum ether (yield: 79%).

### Synthesis of PZLL-DGBE-PZLL

The PZLL-DGBE-PZLL was synthesized as follows: ring-opening polymerization (ROP) of ZLL NCA was carried out in a dried flask with DGBE as an initiator; the reaction mixture was stirred in DMF (10 wt.-%) for 3 d at 30 °C and then precipitated with an excess of diethyl ether under vigorous stirring; then, the viscous polymer was dissolved in chloroform again and precipitated with diethyl ether to give a white solid; and, finally, the product was dried under vacuum at room temperature for 48 h (yield: 87%).

### Characterization of PZLL-DGBE-PZLL

<sup>1</sup>H NMR spectra were measured in D<sub>2</sub>O and in DMSO-d<sub>6</sub> at room temperature (20 ± 1 °C) by an AV-400 NMR spectrometer from Bruker. Molecular weights and their distributions were determined by size exclusion chromatography (SEC) coupled with multiangle laser-light scattering (MALLS). The system included a Styragel HMW6E column, a 515 HPLC pump, an IR OPTILAB DSP detector, and a DAWN EOS multiangle laser-light scattering detector (Wyatt Technology). The MALLS operated at 18 angles with a vertically polarized He-Ne laser (laser wavelength of 690 nm). The absolute molecular weight was determined in 10 mmol · L<sup>-1</sup> LiBr solution in DMF at 30 °C at a flow rate of 1 mL · min<sup>-1</sup>.

### Preparation of Micellar Solutions

The copolymer micellar solutions were prepared using a solvent displacement method as described below: The copolymer (10 mg) was first dissolved in DMF (5 mL) in a 50 mL volumetric flask, and 10 mL of de-ionized water was added with gentle agitation. The mixture was transferred to a dialysis bag (cut-off  $\bar{M}_n$  2 000), and was dialyzed against de-ionized water for two d at room temperature.

### Characterization of the Aqueous Solutions

Measurement of the Critical Micelle Concentration (cmc)

The cmcs were measured by fluorescence technique using pyrene as a probe. Pyrene solution (0.1 mg · L<sup>-1</sup> in acetone) was added into a series of volumetric flasks in such an amount that the final concentration of pyrene in each sample solution was 6.0 × 10<sup>-7</sup> mol · L<sup>-1</sup>, equal to the saturation solubility of pyrene in water at 22 °C; then the acetone was removed completely. The micelle solutions with various concentrations of PZLL-DGBE-PZLL were added to each of the flasks and mixed by vortexing. The flasks were thermo-stated at 30–40 °C for about 2 h to reach an equilibrium, and left overnight. Steady-state fluorescence spectra were obtained on a Perkin Elmer LS50B luminescence spectrometer. For fluorescence excitation spectra,  $\lambda_{em} = 391$  nm. The scan rate was 500 nm · min<sup>-1</sup> and the spectral slit opening was 2.5 nm.

Transmission Electron Microscopy (TEM) Measurements

For observation of the size and distribution of the copolymer aggregates, the solution samples (0.2 mg · mL<sup>-1</sup>) were deposited

onto a copper grid, and the solvent water was evaporated at room temperature. TEM measurements were performed on a JEOL JEM-1011 electron microscope operating at an acceleration voltage of 100 kV and a Hitachi H-8100 transmission electron microscope operated at an accelerating voltage of 200 kV.

#### Atom Force Microscopy (AFM) Measurements

AFM measurements were performed with SPI 3800/SPA 300HV (Seiko Instrument Inc.) in tapping mode at room temperature in air. The tip was of OMCL-ACTS-W type. The samples were prepared by spin-coating a drop of dilute aqueous solution onto a silicon wafer at room temperature.

#### Dynamic Light Scattering (DLS) Measurements

DLS measurements were carried out with a DAMN EOS instrument equipped with a He-Ne laser at the scattering angle of 90°. The micelle solution of about 0.4 mg · mL<sup>-1</sup> was filtered before measurement.

#### Confocal Laser Scanning Microscopy (CLSM) Measurements

CLSM images were collected with a Leica TCS SP2 CLSM (Leica Microsystems Heidelberg GmbH, Germany) equipped with an X20 dry objective (NA = 0.7) using digital zooms of 1 to 32× attached to a Leica DM IRE2 inverted microscope. Confocal optical sections were collected in the image-scan x-y-z mode. The samples were excited by using a 543 nm He/Ne laser. A drop of LCM solution containing Rhodamine B was deposited on a glass surface, dried, and visualized directly.

## Results and Discussion

### Synthesis and Characterization of PZLL-DGBE-PZLL

It has been demonstrated that poly( $\alpha$ -amino acid)s can be prepared by ROP of NCA via a nucleophilic addition with a nucleophilic initiator such as alcohols, amines, and transition-

metals.<sup>[21]</sup> In the present study, a small molecular diamine DGBE was used as the initiator. Figure 1 shows the <sup>1</sup>H NMR spectrum of PZLL-DGBE-PZLL in DMSO-d<sub>6</sub>. All characteristic resonances in PZLL and DGBE can be found. The peaks at 2.9, 3.8, 4.9, and 7.2 ppm are assigned to the protons of PZLL blocks. The peaks at 3.4, 3.3 and 1.7 ppm are assigned to the protons of DGBE block. This indicates successful ROP of ZLL NCA. The degree of polymerization,  $DP_{PZLL}$ , can be obtained by calculating the integral ratio of phenyl protons (g, 7.2 ppm) to ethylene protons (a, 3.4 ppm). The molecular characteristics of the copolymers are shown in Table 1. As shown in Table 1, the molecular weight of the copolymer increases with the monomer-to-initiator ratio, which indicates that it is a controllable polymerization, although not a truly "living" process.<sup>[21]</sup> The block lengths measured by <sup>1</sup>H NMR are in agreement with the theoretical one, consistent with the GPC results.

### Formation of the Vesicles

It is reported that the secondary conformation of PZLL in water is compact  $\alpha$ -helix because of hydrogen-bonding interaction between the main chains.<sup>[22]</sup> A conventional method is used to prepare its micellar solution. Firstly, the polymer is dissolved in a common solvent (DMF), and then a selective solvent (water) is added. At the very beginning, the system is in a thermodynamic equilibrium because of low water content. With the addition of water, the solvent is exacted from the hydrophobic PZLL. The de-solvated PZLL chains become aggregated. In other words, the PZLL chains become a frozen state from a free state (solvated in DMF solution) in aggregates, being a sort of glass transition at room temperature. Figure 2 shows the morphology of the nano-scale vesicles formed from their solution. From the TEM images, it can be seen that they are spherical and the darkness of the circumference is different from inside; this

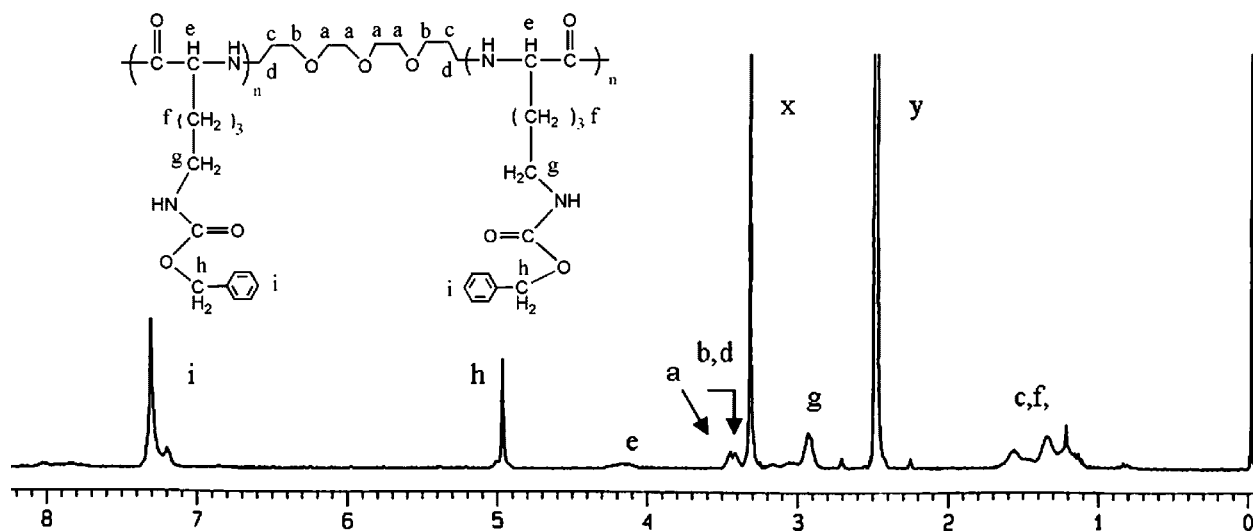
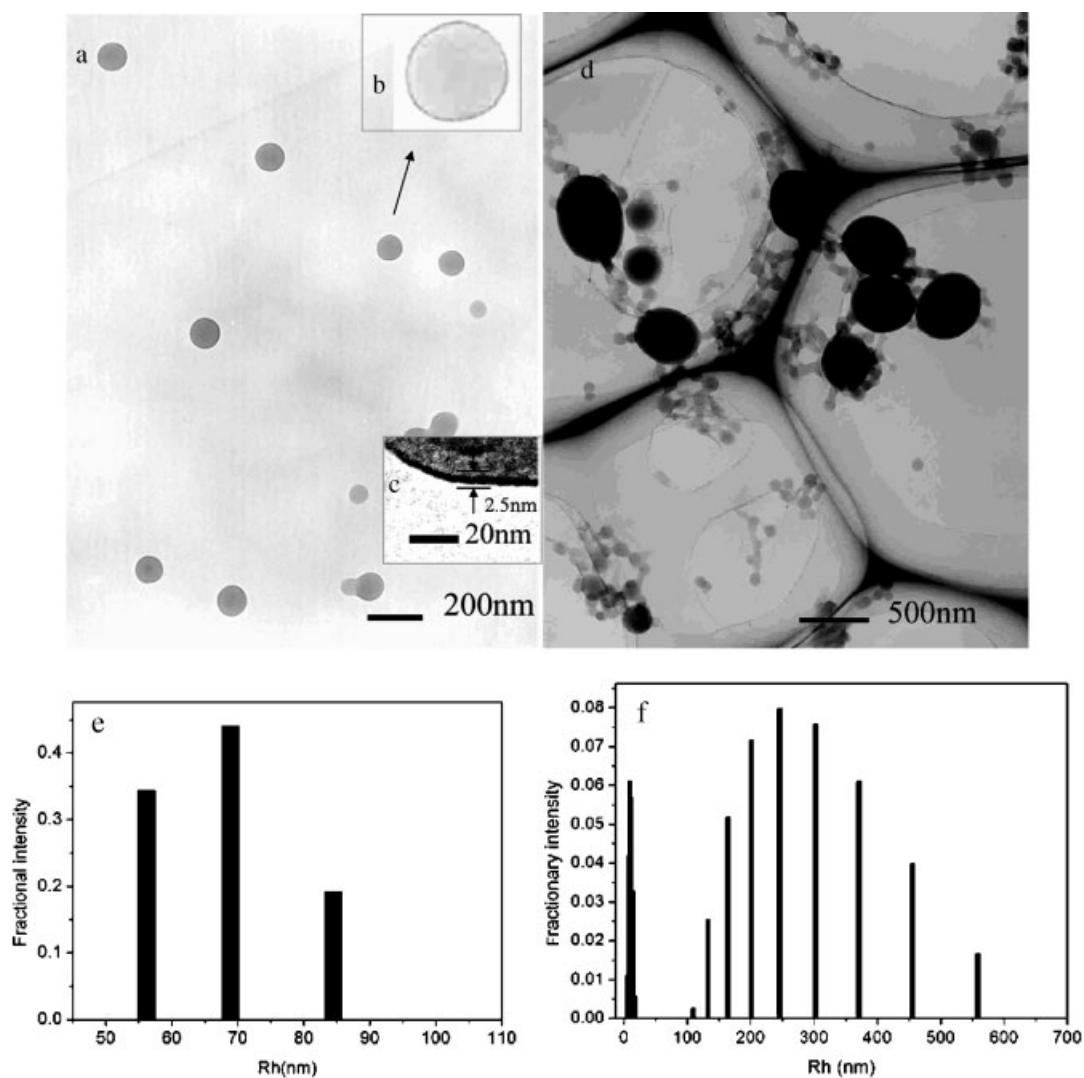


Figure 1. <sup>1</sup>H NMR spectrum and peak assignment of PZLL-DGBE-PZLL in DMSO-d<sub>6</sub>. The peaks x and y originate from the solvent impurities.

**Table 1.** Feed composition and molecular characteristics of triblock copolymer PZLL-DGBE-PZLL.

| Sample | Molar ratio<br>DGBE:ZLL | $\overline{M}_n$ <sup>a)</sup> | $\overline{M}_w$ <sup>b)</sup> | $\overline{M}_w/\overline{M}_n$ <sup>b)</sup> | Observed<br>structure | Size <sup>c)</sup> | $R_h$ <sup>d)</sup>                     | cmc  |
|--------|-------------------------|--------------------------------|--------------------------------|---|-----------------------|--------------------|---|------|
|        |                         | $10^3$                         | $10^3$                         | nm  |                       | nm                 | $10^{-3} \text{ g} \cdot \text{L}^{-1}$ |      |
| P1     | 1:6                     | 1.7                            | 2.1                            | 1.18  | Vesicles              | 76                 | 40.0                                    | 5.25 |
| P2     | 1:10                    | 2.8                            | 3.2                            | 1.01  | Vesicles              | 82                 | 45.5                                    | 1.66 |
| P3     | 1:16                    | 4.2                            | 8.9                            | 1.06  | Vesicles              | 100                | 67.5                                    | 1.32 |
| P4     | 1:60                    | 15.9                           | 28.3                           | 1.01  | Vesicles              | 280                | 161                                     | 1.05 |
| P5     | 1:125                   | 33.1                           | 38.3                           | 1.02  | Vesicles              | 44.5               | 10.5                                    |      |
|        |                         |                                |                                |   | LCMs                  | 310–600            | 281                                     | 0.86 |
| P6     | 1:175                   | 46.0                           | 48.9                           | 1.12  | LCMs                  | 550–1 000          | 380                                     | 0.72 |

<sup>a)</sup>Determined by  $^1\text{H}$  NMR in  $\text{DMSO-}d_6$  solution; <sup>b)</sup>Determined by SEC-MALLS in DMF ( $10 \text{ mmol} \cdot \text{L}^{-1}$  LiBr); <sup>c)</sup>Determined visually from TEM images for the average diameter of the polymer particles prepared from an aqueous solution of  $0.2 \text{ mg} \cdot \text{mL}^{-1}$ ; <sup>d)</sup>Determined from DLS data for the  $R_h$  of the polymer particles prepared from an aqueous solution of  $0.2 \text{ mg} \cdot \text{mL}^{-1}$ .



**Figure 2.** TEM micrograph of: a) P3 in Table 1; b,c) magnification of a vesicle; and, d) P5 in Table 1. DLS graph of the micelle size distribution of: e) P3 in Table 1; and, f) P5 in Table 1.

is characteristic of a vesicle. It can also be seen that all the particles are dispersed very well and almost no cohesion happens during drying. This can be confirmed by DLS result. The hydrodynamic radius ( $R_h$ ) is calculated from the DLS data by the Stokes-Einstein equation, assuming that the aggregates are of sphere shape.<sup>[23]</sup> The average hydrodynamic radii measured by DLS are shown in Table 1. The particle diameters measured by TEM are a little smaller than hydrodynamic diameters measured by DLS. This may be because of the volume swelling in the solution state. The size distributions of micelles are broad for the samples by DLS measurement (Figure 2e). However, the size of most micelles is still close to the mean radii, consistent with that in TEM micrographs.

A pyrene probe is used to prove the vesicle formation of PZLL-DGBE-PZLL in solution. Figure 3 shows the excitation spectra of pyrene in mixture solution. With increasing concentration of solution, the fluorescence intensity increases, accompanied by a red shift from 333 to 339 nm. This is ascribed to the vesicle formation at certain concentration. The pyrene probe is preferentially partitioned into the hydrophobic inner-layer of the vesicle wall. The red shift, of as far as 6 nm, implies the strong hydrophobic nature of PZLL, which is mainly due to the incorporation of the benzyl groups and the compact stacking of the PZLL chains in the vesicle wall. The cmc value is obtained when the intensity ratio  $I_{339}/I_{333}$  is plotted against the solution concentration (Figure 4). As shown in Table 1, the cmc value decreases with increasing PZLL block length, consistent with the enhancement of the hydrophobicity. It also can be seen that the size of vesicles relates to the molecular structure of the copolymers. The vesicle diameter increases from 76 to 280 nm with increasing PZLL block length (degree of polymerization,  $DP$ , from 6 to 60); in short, the longer hydrophobic block length, the larger the vesicle diameter.

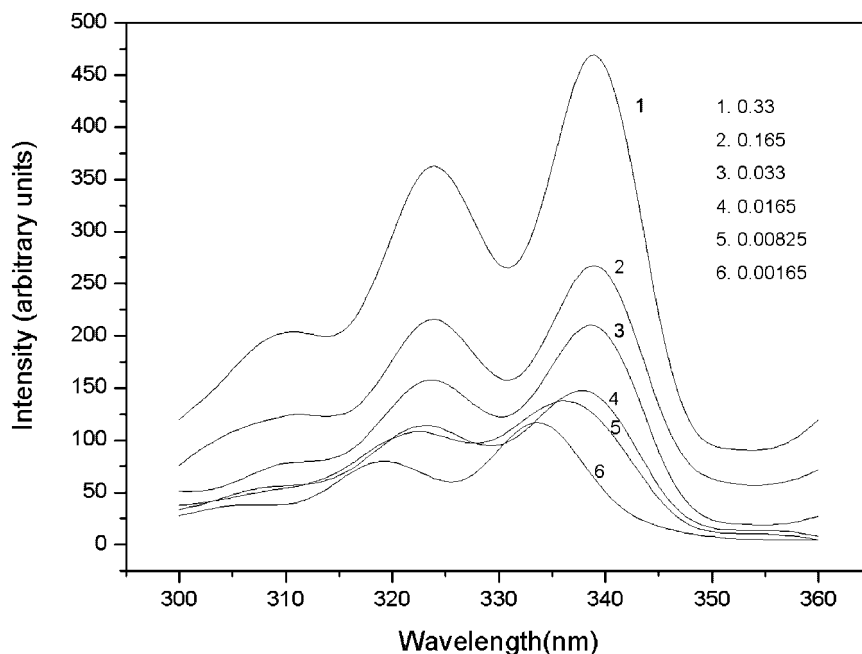


Figure 3. Fluorescence excitation spectra of pyrene in aqueous PZLL-DGBE-PZLL (P2) solutions (concentration in  $\text{g} \cdot \text{L}^{-1}$ ) at room temperature. The emission wavelength was set to 391 nm.

#### Formation of Large Compound Micelles (LCMs)

It has been reported that there are three factors for a force balance to control the morphologies:<sup>[16]</sup> stretching of the core-forming blocks; repulsive interaction among the corona chains; and, surface tension at the core-corona

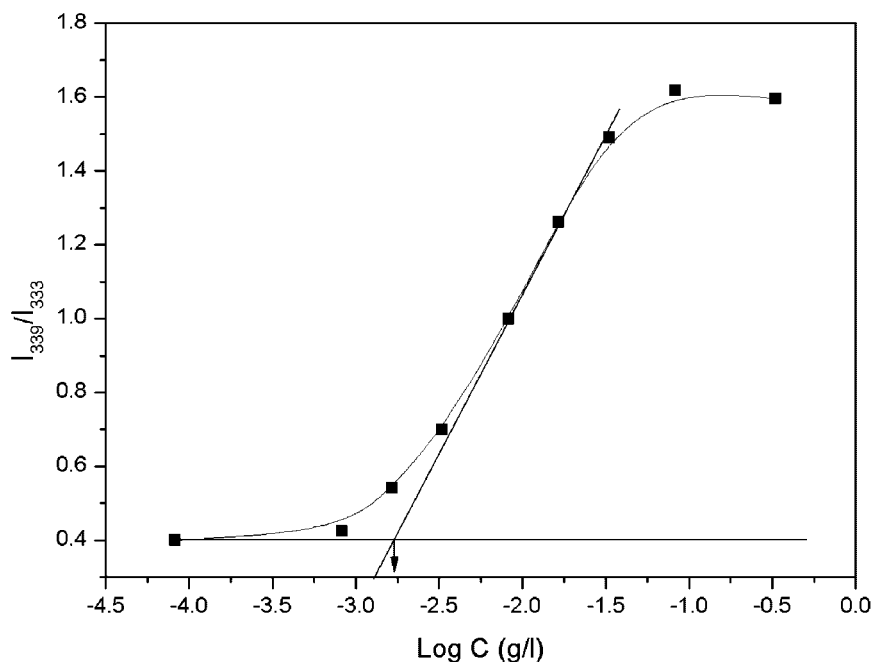


Figure 4. Plot of  $I_{339}/I_{333}$  of pyrene vs.  $\log C$  of the polymer (P2) in de-ionized water.

interface at the onset of micellization. Of them, the contribution of the core may be the most valuable. For our system, the PZLL as a hydrophobic segment forms the inner-layer of the wall in the vesicle. When PZLL block length increases from 6 to 60, the degree of stretching of the PZLL chains will increase correspondingly. For the PZLL block length 6, the vesicles have a wall thickness of ca. 1.2 nm; when the PZLL block length increases to 60, the wall thickness increases to ca. 8.0 nm. In Figure 2c, it can be seen clearly that the wall thickness is about 2.5 nm, consistent with the calculated value.<sup>[24]</sup> When the PZLL block length increases to 125, besides nano-scale vesicles, other morphology appears, that is, large compound micelles (LCMs) (Figure 2d). Different morphologies often coexist.<sup>[25]</sup> In Figure 2f, the DLS graph also shows size distribution over two regions: below 50 nm ( $R_h$ ) and over 100–600 nm ( $R_h$ ). With the PZLL block length further increasing to 175, the LCMs take up the main morphology of the aggregates in solution. They are different from vesicles in their bigger size and wider size dispersion as shown in Figure 5a. DLS data confirm the TEM result (Figure 5b). Furthermore, there is no darkness difference between the circumference and the center. In the height image of AFM (Figure 5c), the particle height is estimated to be ca. 400 nm, comparable with the width. There is no collapse. These observations imply that the dried LCMs are spherical solid particles. We also use Rhodamine B as a probe to get more information on the interior of the LCMs. It is a hydrophilic fluorescent dye and its red fluorescence can be easily seen under CLSM.<sup>[26]</sup> 0.5 mg Rhodamine B was mixed with 5 mg copolymer in 5 mL DMSO and stirred for 24 h. Then 2 mL de-ionized water was added to the mixture dropwise and dialyzed against de-ionized water for 10 h. The hydrophobic nature of the amphiphilic vesicles prevented the penetration of hydrophilic solutes.<sup>[27]</sup> So the LCMs with the inclusion of the hydrophilic dye were prepared. Figure 6 shows the CLSM image of the LCMs formed. It

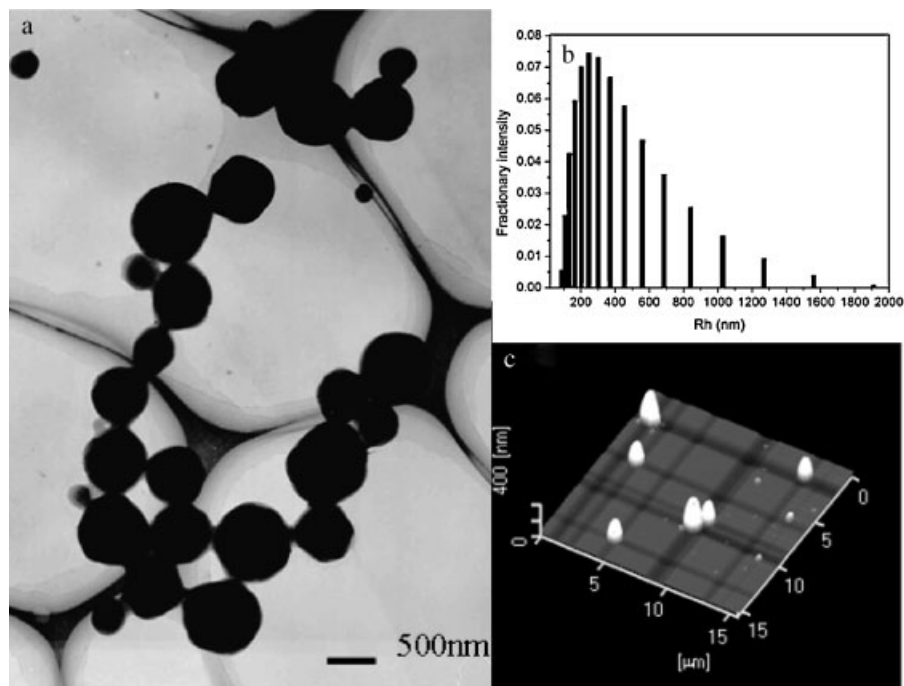


Figure 5. The LCM images from P6: a) TEM micrograph; b) DLS graph of the particle size distribution of P6 in Table 1; and, c) AFM 3-D image.

can be clearly seen that the red fluorescence of Rhodamine B is coming from the aqueous interior of the aggregates, implying that there exist many reverse micelles with aqueous cores in the LCMs. Some precipitates appear in the bottom of solution several days after preparation. However, they can dissolve again in the solution with gentle hand shaking; this may be due to the gravity effect of big solid spheres. The Eisenberg group has researched the inner structure of the LCMs particularly. Their starting copolymers are diblock copolymers such as PS-PAA with  $DP_{PS-PAA} = 200-4$  or  $420-21$ , in which the lengths of the

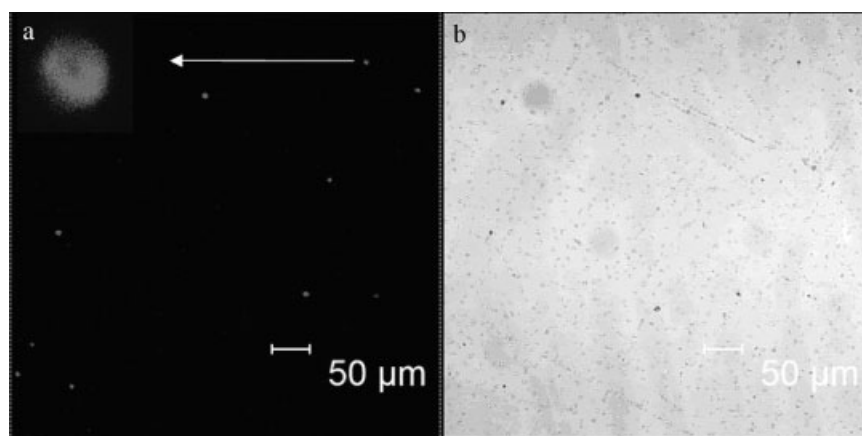
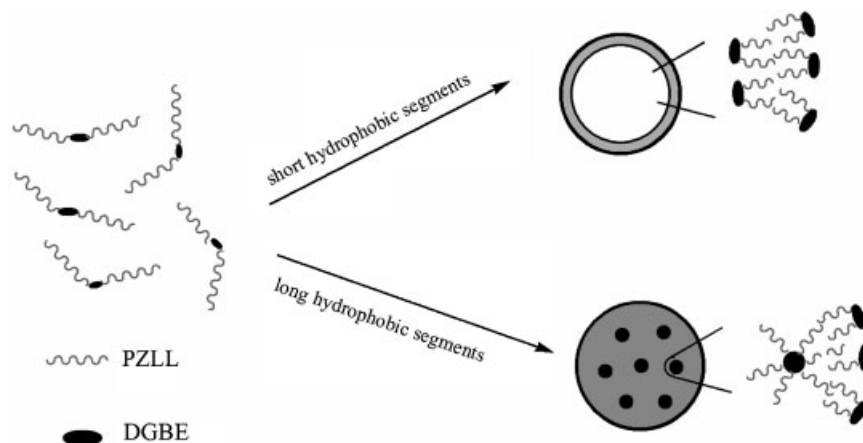


Figure 6. a) CLSM image of the LCM from P6 containing Rhodamine B; b) Bright field images of the LCM.



■ Scheme 1. Formation of vesicle and LCM from block copolymers PZLL-DGBE-PZLL.

both blocks are not comparable, and PS-PEO with  $DP_{PS}=240$  and  $DP_{PEO}=180$ , in which the lengths are comparable. In the present study, the starting polymer is PZLL-DGBE-PZLL. The DGBE block, as a middle block, is relatively short compared to PZLL blocks in general, and it is much shorter than PZLL in the case of P5 and P6 in Table 1 in particular; with increasing chain length of PZLL, the dimension of the wall inner-layer increases. It can not keep enlarging because the short hydrophilic block cannot protect the hydrophobic wall of the vesicle any more, and the long PZLL chains tend to form compact  $\alpha$ -helical aggregates. Consequently, a structure of large compound micelles is formed from PZLL-DGBE-PZLL with further longer PZLL blocks, to minimize the total energy of the whole system. Compared with the similar chain length of PS-PAA,<sup>[16]</sup> the size of LCM for our system is smaller. This is ascribed to the compact  $\alpha$ -helical stacking of the PZLL chains. The LCM structure is illustrated in Scheme 1. It is composed of several reverse micelles covered by a surface layer. The reverse micelles contain a DGBE core and a PZLL corona, and the surface layer is a monolayer of PZLL-DGBE-PZLL, in which the DGBE segments are facing outwards and the PZLL segments are mixed with the one in the reverse micelles. In this way, the LCMs can disperse in aqueous solution with good stability.

## Conclusion

A series of polypeptides PZLL-DGBE-PZLL were synthesized by ROP of ZLL NCA with a small molecular diamine DGBE as the initiator.  $^1\text{H}$  NMR and SEC-MALLS studies confirmed its chemical structure. It can self-assemble into vesicles and/or large compound micelles in aqueous media depending on the PZLL block length. The cmc value decreases with increasing hydrophobic PZLL block length.

This kind of polypeptides is expected to be a novel and promising vehicle for drug delivery.

Acknowledgements: Financial support was provided by the *National Natural Science Foundation of China* (Project Nos. 50373043 and 20674084), the *National Fund for the Distinguished Young Scholars* (No. 50425309) and the *Chinese Academy of Sciences* (Project No. KJCX2-SW-H07).

Received: January 13, 2008; Revised: March 1, 2008; Accepted: March 3, 2008; DOI: 10.1002/macp.200800018

Keywords: large compound micelles; *N*-carboxyanhydride (NCA); polypeptides; self-assembly; vesicles

- [1] P. Papadopoulos, G. Floudas, I. Schnell, T. Aliferis, H. Latrou, N. Hadjichristidis, *Biomacromolecules* **2005**, *6*, 2352.
- [2] A. Finne, N. Andronova, A. C. Albertsson, *Biomacromolecules* **2003**, *4*, 1451.
- [3] S. Caillol, S. Lecommandoux, A. F. Mingotaud, M. Schappacher, A. Soum, N. Bryson, R. Meyrueix, *Macromolecules* **2003**, *36*, 1118.
- [4] D. M. Tang, J. P. Lin, S. L. Lin, S. Zhang, C. Tao, X. H. Tian, *Macromol. Rapid Commun.* **2004**, *25*, 1241.
- [5] M. Muthukumar, C. K. Ober, E. L. Thomas, *Science* **1997**, *277*, 1225.
- [6] A. Kros, W. Jesse, G. A. Metselaar, J. J. L. M. Cornelissen, *Angew. Chem. Int. Ed.* **2002**, *8*, 41.
- [7] F. Chécot, S. Lecommandoux, Y. Gnanou, H. A. Klok, *Angew. Chem. Int. Ed.* **2005**, *44*, 4349.
- [8] A. P. Nowak, V. Breedveld, L. Pakstis, B. Ozbas, D. J. Pine, D. Pochan, T. J. Deming, *Nature* **2002**, *417*, 424.
- [9] J. Sun, C. Deng, X. S. Chen, H. J. Yu, H. Y. Tian, J. R. Sun, X. B. Jing, *Biomacromolecules* **2007**, *8*, 1013.
- [10] C. B. Mao, D. J. Solis, B. D. Reiss, S. T. Kottmann, R. Y. Sweeney, A. Haryhurst, G. Georgiou, B. Iverson, A. M. Belcher, *Science* **2004**, *303*, 213.
- [11] A. J. Dirks, S. S. Berkel, N. S. Hatzakis, J. A. Opsteen, F. L. Delft, J. J. L. M. Cornelissen, A. E. Rowan, J. C. M. Hest, F. P. J. T. Rutjes, R. J. M. Nolte, *Chem. Commun.* **2005**, 4172.

- [12] M. Matsusaki, T. Waku, T. Kaneko, T. Kida, M. Akashi, *Langmuir* **2006**, *22*, 1396.
- [13] F. Chécot, S. Lecommandoux, Y. Gnanou, H. A. Klok, *Angew. Chem. Int. Ed.* **2002**, *41*, 1339.
- [14] E. P. Holowka, D. J. Pochan, T. J. Deming, *J. Am. Chem. Soc.* **2005**, *127*, 12423.
- [15] A. Koide, A. Kishimura, K. Osada, W. D. Jang, Y. Yamasaki, K. Kataoka, *J. Am. Chem. Soc.* **2006**, *128*, 5988.
- [16] L. F. Zhang, A. Eisenberg, *Science* **1995**, *268*, 1728.
- [17] K. Yu, A. Eisenberg, *Macromolecules* **1996**, *29*, 6359.
- [18] K. Yu, A. Eisenberg, *J. Am. Chem. Soc.* **1997**, *119*, 8383.
- [19] K. R. Brzezinska, S. A. Curtin, T. J. Deming, *Macromolecules* **2002**, *35*, 2970.
- [20] W. H. Daly, D. Poché, *Tetrahedron. Lett.* **1988**, *29*, 5859.
- [21] H. R. Kricheldorf, "α-Aminoacid-N-Carboxy-Anhydrides and Related Heterocycles", Springer-Verlag, Berlin 1987.
- [22] C. S. Cho, B. W. Jo, J. K. Kwon, T. Komoto, *Macromol. Chem. Phys.* **1994**, *195*, 2195.
- [23] C. Wu, B. Chu, *Macromolecules* **1994**, *27*, 1766.
- [24] K. T. Kim, C. Park, G. W. M. Vandermeulen, D. A. Rider, C. Kim, M. A. Winnik, I. Manners, *Angew. Chem. Int. Ed.* **2005**, *44*, 7964.
- [25] A. Wittmann, T. Azzam, A. Eisenberg, *Langmuir* **2007**, *23*, 2224.
- [26] R. Donohue, A. Mazzaglia, B. J. Ravoo, R. Darcy, *Chem. Commun.* **2002**, 2864.
- [27] A. Koide, A. Kishimura, K. Osada, W. D. Jang, Y. Yamasaki, K. Kataoka, *J. Am. Chem. Soc.* **2006**, *128*, 5988.